ONSET VOLTAGE OF NEGATIVE CORONA ON STRANDED CONDUCTORS

M. M. EL-Bahy, M. Abouelsaad, N. Abdel-Gawad and M. Badawi

Faculty of Engineering, Benha University, Cairo, Egypt

Theoretical investigation of the onset voltage of negative corona on stranded conductors is described in this paper. The method of calculation is based on the criterion developed for the formation of repetitive negative corona Trichel pulses. This calls at first for accurate calculation of the electric field in the vicinity of stranded conductors. The investigated gap is a three dimensional field problem. To solve this problem, a new modification of the charge simulation technique (CST) is presented, where the simulation charges are helical of infinite length. Laboratory measurements of the onset voltage on stranded conductors are carried out to check the accuracy of the present calculations. The effects of varying the field nonuniformity on the onset voltage values are investigated. The calculated onset voltage values for stranded conductors agree satisfactorily with those measured experimentally.

1. INTRODUCTION

Corona can limit the performance of any given configuration of electrical conductors [1]. Hence, the onset voltage of the corona is an important design consideration for any set of stressed conductors. Knowledge of this voltage is of paramount importance in gas insulated systems. The problems associated with the corona discharge on HV transmission line conductors are power loss, audible noise and electromagnetic interference [2]. These problems can limit the voltage to which the line can be energized.

Gas insulated substations (GIS) are successfully used for high-voltage ac power systems. With the tremendous increase of power transmitted, dc transmission becomes competitive and many dc transmission lines are installed everywhere in the world [3]. This has created a growing interest in the study of self-maintained corona discharge on dc transmission lines. Onset corona fields on smooth round conductors for both polarities are believed to be approximately equal and in agreement with experiment, within the limits of experimental error [4]. Hence, in this paper onset voltage of corona may be predicted by calculating the onset voltage of negative polarity.

The corona onset voltage for a smooth round conductor in atmospheric air is well described by simple empirical formulae based on experimental data [5,6]. These formulae are of great benefit because the onset corona field E_o can

be calculated for any radius without much numerical calculations. However, at normal pressure and temperature, these formulae predict values of E_o that vary widely for the same gap geometry and are given for both polarities by Lowke et al as [4] :

$$E_o \ (\ \mathrm{kVcm^{-1}} \ ) = 25 \ (\ 1 + \frac{0.4}{\sqrt{R}} \ ), \tag{1}$$

Also, another empirical formula has been presented in [5],

$$E_o \ (\ \mathrm{kVcm^{-1}} \ ) = A \ + \ \frac{B}{\sqrt{R}} \tag{2}$$

where, R is the conductor radius in cm, A and B lie in the ranges 29.4 to 40.3 and 7.34 to 9.92, respectively, for negative polarity [5], Peek [6] reported A and B as equal to 31, 9.55.

Practical transmission lines are normally of stranded construction and often contain surface irregularities. Stranded conductors are composed of 7, 19, 37,…etc strands in continuing fixed increments and the external layer twists around interior layers in helical (spiral) form. Conductors are stranded mainly to increase their flexibility with a subsequent increase of the mechanical strength. Stranding distorts the field in the immediate vicinity of the conductor and reduces the corona onset voltage. The influence of stranding on the corona onset voltage of smooth round conductor was investigated experimentally many years ago by Peek [6]. He characterized the influence of the strands by introducing a surface irregularity factor, m, defined as the ratio of the corona onset voltage of a stranded conductor to that of a smooth round conductor with the same outer diameter. The value of m equals unity for a perfectly smooth conductor, and is less than 1 for stranded conductors. Peek gave m a range of 0.72 to 0.82 for 7 stranded conductors. In Whitehead's investigation [7], the number of strands in the outer layer, no, was varied from 3 to 9. His data for m ranged from 0.85 to 0.92 and illustrated the physically intuitive result that conductors with a large number of strands behaved more like smooth conductors than conductors with a small number of strands. Hence, there are no definite values of m and onset voltage. In addition, the onset voltage depends not only on the value of the surface field but also on the field distribution in the vicinity of the conductor and the properties of the gas in which the conductor is located. Therefore, the empirical formulae predict inaccurate values of onset voltage of corona. This motivates the authors to conduct the present study.

The main target of this paper aims to investigate the effect of stranding on the onset voltage of negative corona on stranded conductors positioned in air opposite to a ground plane. The onset voltage calculation is based on the criterion developed for the formation of repetitive negative corona Trichel pulses. This criterion calls for the assessment of the electric field in the vicinity of the stressed conductor. The accurate CST is used for field calculation in the vicinity of the stressed conductors. As the external layer twists around the

interior layers in a helical shape, the simulating charges take the same helical form. To the best of our knowledge, the helical charge has not yet been reported in literature. Also, laboratory measurements of the onset voltage of corona on 7-stranded conductors are carried out. The effects of varying the field nonuniformity on the onset voltage values are investigated. The calculated onset voltage values for stranded conductors are compared with those measured experimentally and with values obtained by empirical formulae.

2. TWISTING OF EXTERNAL LAYER OF STRANDED CONDUCTOR

The outer layer of stranded conductors twists around the inner layers in a helical form. The locus of a point a(x, y, z) which moves in a uniform motion along a generatrix around circular conductor is called a helix [8]. The length of one complete revolution of a point a(x, y, z), around the conductor axis is called a pitch and it is repeated along the helix. Practically, the pitch length (L_p) equals the pitch factor (*PF*) times the overall diameter (2R) of the stranded conductor [9] and *PF* for 7, 19 and 37 stranded conductors equals 16-18, 14-16 and 12-14, respectively [9]. Hence, $L_p = 2R \times PF$, where, *PF* is chosen to be 17, 15 and 13 for 7, 19 and 37 stranded conductors, respectively. The location of point a(x, y, z) is related to L_p and the conductor radius R.

3. METHOD OF ANALYSIS

3.1. Electric Field Calculation around Stranded Conductor

The analysis is based on CST in which the distributed charges on the surface of the stressed conductor are replaced by a set of fictitious simulation charges arranged inside the external layer of stranded conductors. To maintain the ground plane at zero potential, images of the simulation charges are considered. Satisfaction of the pertinent boundary condition results a set of equations whose simultaneous solution determines the unknown simulation charges. Knowing the simulating charges, the electric potential and field can be calculated at any point in the investigated gap.

3.1.1. Simulation technique

The simulating charges are placed inside each strand of the external layer and take the same helical shape of the strand and repeat along the x-axis after a pitch. The stranded conductor is assumed infinitely long and segmented into infinite number of pitches (-∞,..., -k,...,-1, 0, 1,...k,..., ∞). The number of simulating helical charges, (q_h), is assumed to be 3 times of the number of strands in the outer layer (*3 $\times$ n_o*). In each pitch, any helical charge is divided

into n finite line charges; having length (1), and equal projections along x-axis, Figure (1). Hence, the number of simulating finite line charges in each pitch equals N, ($N = 3 \times n \times n_o$), however, only the unknown simulating charges are those in pitch-0 because the pitches are repeated. Each finite line charge inclusive of its image will be assigned to a Cartesian co-ordinate systems (x_1, y_1, z_1) and (x_2, y_2, z_2), respectively [10]. By transformation of co-ordinates, an arbitrary point $A_i(x, y, z)$ is referred to these new coordinates. A coordinate transformation will be conducted for the complete arrangement of simulation line charges.

3.1.1.1. Coordinates of simulating finite line charges

Figure (2) shows a cross section of 7 stranded conductor which has $n_o = 6$, overall radius R and the gap height H. Inside each strand of the outer layer, the three simulation helical charges q_{h1}, q_{h2} and q_{h3} in the y-z plane are assumed to be spaced radially from the strand center by distances $f_1 R_s$, $f_2 R_s$ and $f_3 R_s$ where, R_s is the strand radius, f_1, f_2 and f_3 are fractions greater than 0 and less than 1. The angle ψ defines the relative angular positions of q_{h2} and q_{h3}.
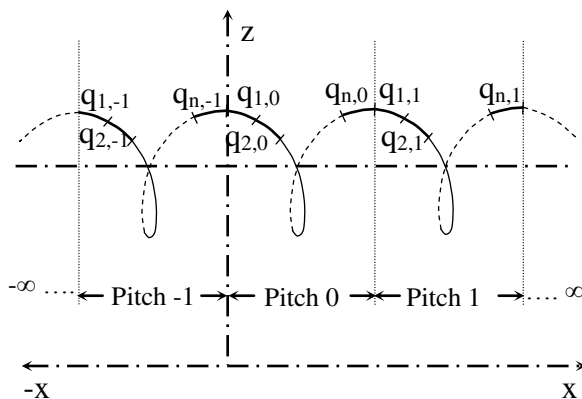

Figure 1: Division of the helical charge, q_h, into infinite number of pitches (-∞,…, -k ,…,-1,0,1,…k,…, ∞) and division of that charge in each pitch into n finite line charges.

3.1.1.2. Coordinates of boundary points

To satisfy the boundary conditions, a boundary point is chosen on the strand surface corresponding to each finite line charge. Hence, N boundary points are chosen for pitch-0 on the stranded conductor surface. Each boundary point lies on its loci at the middle of the corresponding simulation line charge, Figure 2.
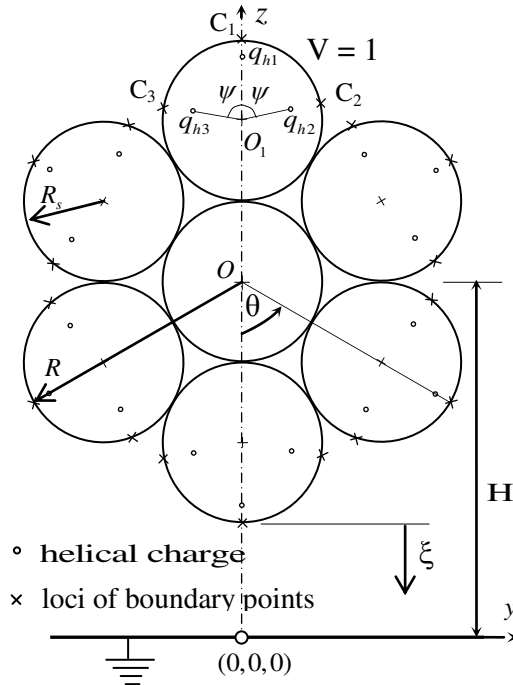
Figure 2: The location of helical charges and contour points loci in cross section of 7 stranded conductor.

3.1.2. Potential Calculation

The potential ϕ_i at an arbitrary contour point $A_i(x, y, z)$, due to the simulation line charges Q_j, ($Q_j = q_{j,0}, j = 1, 2, …, N$), is calculated by the relation

$$\phi_i = \sum_{j=1}^{j=N} P_{i,j} \, Q_j \tag{3}$$

where, $P_{i,j}$ is the summation of potential coefficients $p_{i,j,k}$ at the point $A_i(x, y, z)$ due to all simulation line charges,

$$P_{i,j} = \sum_{k=-\infty}^{k=\infty} p_{i,j,k} \tag{4}$$

where, the potential coefficient $p_{i,j,k}$ is expressed as [11]

$$p_{i,j,k} = \frac{1}{4\pi\varepsilon 1_j} ln\left(\frac{\left[(1_j - x_{1j}) + \gamma_{1j}\right]}{\left[(-x_{1j}) + \delta_{1j}\right]} \frac{\left[(-x_{2j}) + \gamma_{2j}\right]}{\left[(1_j - x_{2j}) + \delta_{2j}\right]} \right) \tag{5}$$

where,

$$\gamma_{1j} = \sqrt{(1_j - x_{1j})^2 + y_{1j}^2 + z_{1j}^2}, \quad \gamma_{2j} = \sqrt{x_{2j}^2 + y_{2j}^2 + z_{2j}^2}$$

$$\delta_{1j} = \sqrt{x_{1j}^2 + y_{1j}^2 + z_{1j}^2}, \quad \delta_{2j} = \sqrt{(1_j - x_{2j})^2 + y_{2j}^2 + z_{2j}^2}$$

Equating the applied voltage with the calculated potential at the selected boundary points results in a set of equations whose solution determine the unknown simulation charges.

3.1.3. Electric Field Calculation

It is well known that, the electric field intensity E is the negative gradient of the potential. The differentiation of potential ϕ_i in the coordinate systems (x_1, y_1, z_1) and (x_2, y_2, z_2) is conducted separately. Thus the components of the electric field, $(E_{x1i,j}, E_{y1i,j}, E_{z1i,j}, E_{x2\,i,j}, E_{y2\,i,j}$ and $E_{z2\,i,j})$, of charge Q_j and its image in the co-ordinate systems (x_1, y_1, z_1) and (x_2, y_2, z_2) are obtained, respectively. These components must be transformed back and added into the main co-ordinate system (x, y, z). Hence, for each finite line charge Q_j and its image, at a contour point $A_i(x, y, z)$, the field intensity components $E_{xi,j}$, $E_{yi,j}$ and $E_{zi,j}$ are

$$
\begin{aligned}
E_{x\,i,j} &= (E_{x1\,i,j} + E_{x2\,i,j})\cos\delta_j \cos\beta_j \\
&\quad - (E_{y1\,i,j} + E_{y2\,i,j})\sin\beta_j \\
&\quad - (E_{z1\,i,j} - E_{z2\,i,j})\sin\delta_j \cos\beta_j
\end{aligned}
$$

$$
\begin{aligned}
E_{y\,i,j} &= (E_{x1\,i,j} + E_{x2\,i,j})\cos\delta_j \sin\beta_j \\
&\quad + (E_{y1\,i,j} + E_{y2\,i,j})\cos\beta_j \\
&\quad - (E_{z1\,i,j} - E_{z2\,i,j})\sin\delta_j \sin\beta_j
\end{aligned}
$$

$$
\begin{aligned}
E_{z\,i,j} &= (E_{x1\,i,j} - E_{x2\,i,j})\sin\delta_j \\
&\quad + (E_{z1i,j} + E_{z2\,i,j})\cos\delta_j
\end{aligned}
\tag{6}
$$

where, the angles δ_j and β_j are the inclination angles of a line charge having length, 1_j, on x-y and x–z planes, respectively, as shown in Figure 3.

Hence, the field intensity components E_{xi}, E_{yi}, and E_{zi} at point $A_i(x, y, z)$ are obtained as follows:

$$
E_{xi} = \sum_{j=1}^{j=N} E_{x\,i,j}
$$

$$
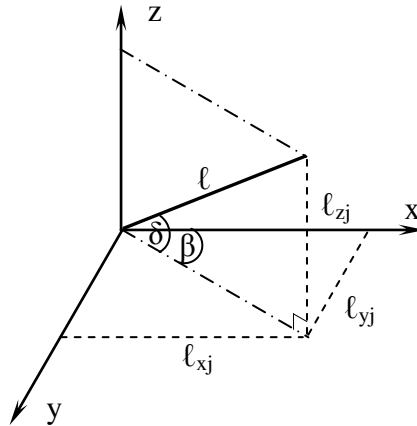E_{yi} = \sum_{j=1}^{j=N} E_{y\,i,j}
$$

$$
E_{zi} = \sum_{j=1}^{j=N} E_{z\,i,j}
$$

Figure 3: The inclination angles δ_j and β_j of line charge having length, 1_j on x-y and x–z planes, respectively

Then, the field intensity at that point is calculated by the relation

$$E_i = \sqrt{E_{xi}^2 + E_{yi}^2 + E_{zi}^2} \tag{7}$$

4. ONSET CRITERION OF NEGATIVE CORONA

When the electric field strength in the vicinity of the stranded conductor surface reaches the onset value for ionization of air molecules by electron collision, a primary avalanche starts to develop along the gap axis away from the conductor, Figure (4); where the field assumes maximum values. With the growth of the avalanche, more electrons are developed at its head, more photons are emitted in all directions, and more ions that are positive are left in the avalanche's wake. The avalanche growth takes place under the combination of the field due to the applied voltage and the field of the positive ions in the wake of the avalanche itself. The growth of the avalanche continues as long as Townsend's first ionization coefficient, $\alpha(\xi)$, is greater than the electron attachment coefficient, $\eta(\xi)$, and terminates at z = Z_i; i.e. at the ionization-zone boundary, $(\alpha(\xi) = \eta(\xi))$ [12], where, the electrons get attached to the air molecules and form negative ions.

For a successor avalanche to be started, the preceding avalanche should some how provide an initiating electron at the stressed electrode surface, possibly by photoemission, positive ion impact, metastable action, or field emission. Field emission is possible only at field strengths exceeding 5×10^7 V/m. Electron emission by positive-ion impact is more than two orders of magnitude less frequent than that by photoemission. Metastables have been reported to have an effect approximately equal to that of positive ion impact. Therefore, only the first mechanism (electron emission from the cathode by

photons) was considered in the mathematical formulation of the onset criterion [13], where at least one photoelectron, ($N_{eph}=1$), is emitted by the photons of the primary avalanche to keep the discharge self sustaining [12], i.e

$$N_{eph} = \gamma_{ph} \int_{H-R}^{Z_i} \alpha\ (\xi)\ g\ (\xi) \exp\left[\int_{H-R}^{Z_i} (\alpha\ (\xi) - \eta\ (\xi)) d\xi \right] \exp(-\mu\ \xi\ ) d\xi \qquad (8)$$

where, γ_{ph} is Townsend's second coefficient due to the action of photons, and Z_i is the distance measured along the gap axis determining the ionization-zone boundary, Figure (4) and $g(\xi)$ is a geometric factor to account for the fact that some photons are not received by the cathode [14]; considering the stranded conductor surface as that of a smooth conductor. The condition for a new (successor) avalanche to be developed is

$$N_{eph} \geq 1 \qquad (9)$$

The onset voltage of corona does not appear explicitly in the relation (8). However, the values of α, η which is given in [12] are affected by the applied voltage. The onset voltage is the critical value, which fulfills the equality (9).
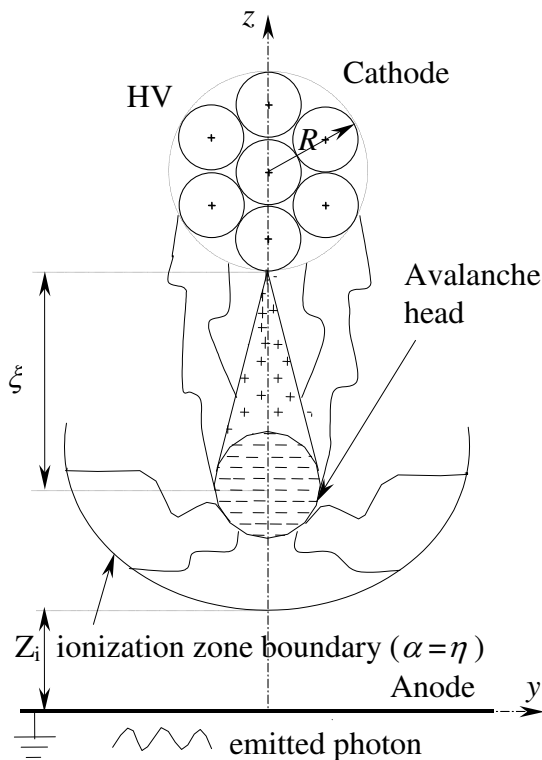

Figure 4: Development of the primary avalanche along the gap axis in negative onset of corona.

5. EXPERIMENTAL SET-UP AND TECHNIQUE

The experiments were carried out in atmospheric air using 7 strand-conductors of outer radii 1, 1.25 and 1.5 mm. Conductor height above the ground plane ranged from 0.11 to 0.56 m. The length and the width of plane electrode are 2 and 1 m, respectively. The plane was grounded through 30 k Ω resistor. A high voltage dc source (Hipotronics, Model 800PL-10MA series) has been employed to energize the stranded conductor up to 80 kV and 10 mA. It has a maximum ripple factor of 2.5%. Overall accuracy of voltage measurement was considered to be within ± 2%. The stressed conductor is connected to the HV source through a water resistance of 1 MΩ as a current-limiting resistor. The voltage drop across the 30 k Ω resistor was fed to an oscilloscope. To determine the corona onset voltage, the applied voltage was raised to about 90% of the expected value at a rate of 1 kV/sec and thereafter at a rate of 0.1 kV/sec until the initiation of corona pulses on the oscilloscope takes place [15]; the applied voltage is the corona onset value. The minimum time interval between two successive applied voltages was 1 minute. At least 10 measurements were taken to get the mean value for each measuring point. The relative standard deviation of the mean values was generally smaller than 1.3 %. The tests have been conducted in laboratory air at room temperature (about 22-25º C), atmospheric pressure and low humidity.

6. RESULTS AND DISCUSSION

To check the accuracy of the charge simulation, check points are selected over the conductor circumference which lies midway between two successive boundary points on the same locus. The potential and the deviation angle of the field at the conductor surface are assessed at the check points to check how well the boundary condition is satisfied. This check was made for practical ranges of 7,19, and 37 stranded conductors' radii. These radii ranges are respectively 1 to 6.5, 4.5 to 11.4, and 7.5 to 12.5 mm [9]. The accuracy remained the same for these investigated ranges as given for samples computed at a conductor height H = 1m from the earthed plane.

The accuracy of a simulation depends strongly on the assumptions concerned with the choice of the number and coordinates of the simulation charges. In pitch-0, the number of the finite line charges was assumed to be $N = 3n \times n_o$. The best value of n was found to be 40. Hence, N = 720, 1440 and 2160 for 7, 19 and 37 stranded conductors, respectively. The effective number of pitches (*1+2k*) for these stranded conductors was found to depend on the gap height H, wherever the best value of *k* was found to be integer of (80 H + 12), i. e. for H = 1 m, *k* will be 92 pitch. As a result the effective length achieving the simulation accuracy of the stranded conductor will be equal to *[1+2× (80 H + 12)] ×2R×PF*. It depends on the gap height, conductor radius and type of

stranding. Also, the accuracy of a simulation was found to be highly influenced by the variables f_1, f_2 and angle ψ . Acceptable accuracy is achieved when these factors take values of (0.23, 0.5 and 109°), (0.17, 0.17 and 60°) and (0.22, 0.22 and 75°) for 7, 19 and 37 stranded conductors, respectively.
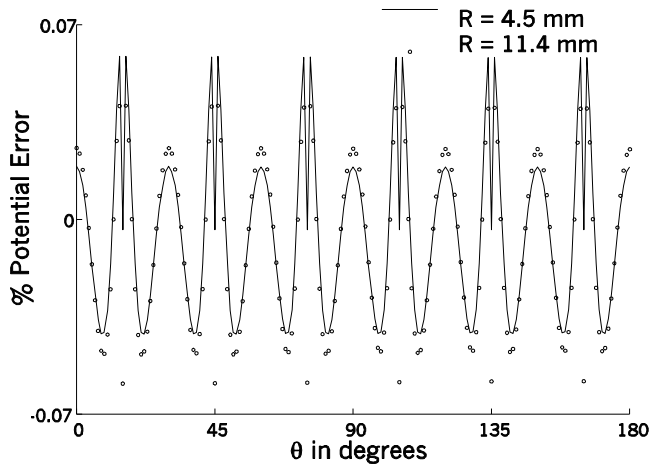
At the circumference of check points, the percentage errors of the potential and the electric field deviation angle in y-z plane are calculated. Figure 5 shows the percentage errors of the calculated potential for 7,19 and 37 stranded conductors. The maximum per cent error does not exceed 0.07%. Potential errors on the electrode surface of less than 0.1 % are considered reasonable for accurate field solution [16]. Over most of the stranded conductor surfaces, (except narrow zones that lie near the contact points of the outer layer strands),   the electric field deviation angle does not exceed 3, 3.4 and 1.3 degrees for 7, 19 and 37 stranded conductors, respectively. As shown in figure 6, the field values near the contact points of the outer layer strands is very low (5.8, 1.2 against 189.6, 38.3 kV/m around the conductor circumference for R = 1 and 6,5 mm, respectively,), hence, the error near these points has no effect on the onset voltage of corona.

Figure 7 gives an example of the electric field distribution near the stressed conductor for smooth and stranded conductors with different values of n_o. Two properties of these results should be noted. First, the maximum values of the surface electric field divided by the maximum value for smooth round conductor (E_{pu}) for n_o = 6, 12 and 18 strands, equals 1.415, 1.43 and 1.441, respectively, against values 1.407, 1.436 and 1.445 obtained theoretically before using conformal mapping, for the same radius and gap height [17]. These values indicate that the surface field is nearly independent of n_o and is in agreement with previous investigators [1,18] who assigned 1.4 for the value of E_{pu}, i.e. independent of n_o. Second, the larger n_o, the smaller the region over which the electric field deviates from that of a smooth conductor, that region approaches zero as $n_o \rightarrow \infty$. This explains why the corona onset voltage for n_o = 18 is greater than both onset voltage values for n_o = 6 and 12 and approaches that of a smooth round conductor, Figure (8).

The surface irregularity factor m was calculated for various numbers of strands in the outer layer n_o at varying conductor radius, R and the gap height, H as shown in Figure 9. At gap height H = 1m, this factor decreases with an increase of conductor radius over the range 1 to 20 mm, Figure 9-a. The decrease of this factor is smaller in the case of R = 10 mm and H varies from 0.1 to 1 m. Also, it is shown that as n_o increases m approaches the value of a smooth round conductor (m = 1) and it has a definite value at certain conductor radius, gap height and number of strands in the outer layer n_o.
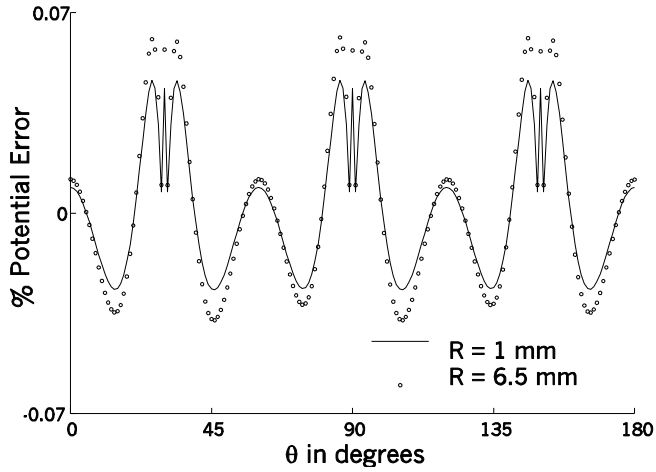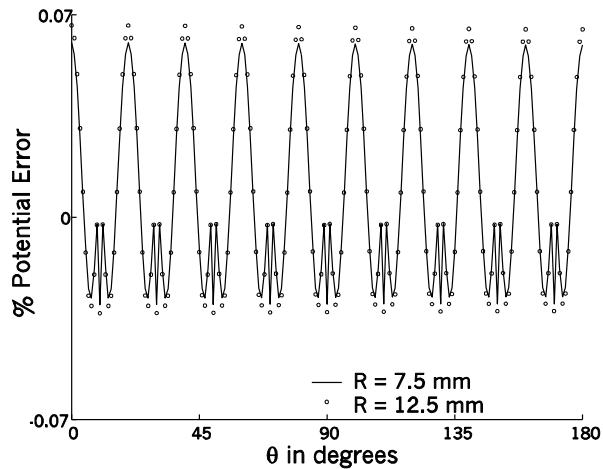
Figure 5: The variation of per cent potential errors at the check points around the circumferences of practical 7,19, and 39 stranded conductors, respectively.
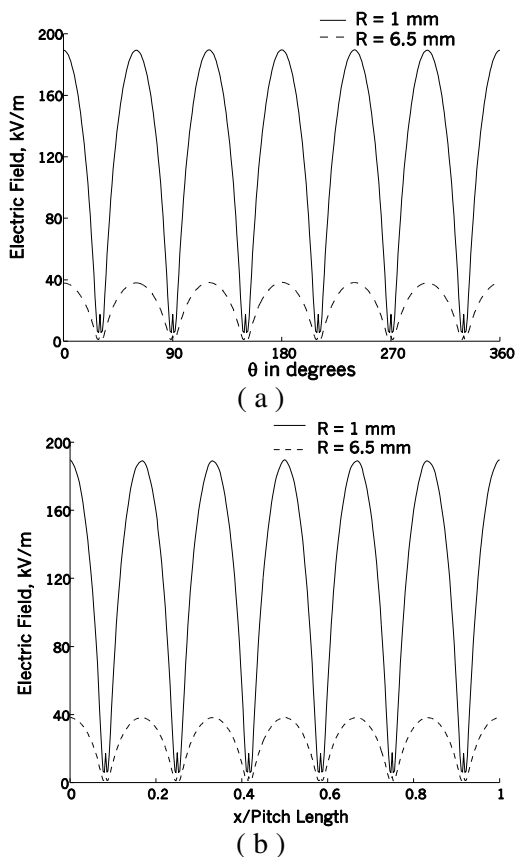
Figure 6: Electric field distribution for 7-strand conductors; (a) around the conductor circumference (b) along the pitch length at the line facing the ground.
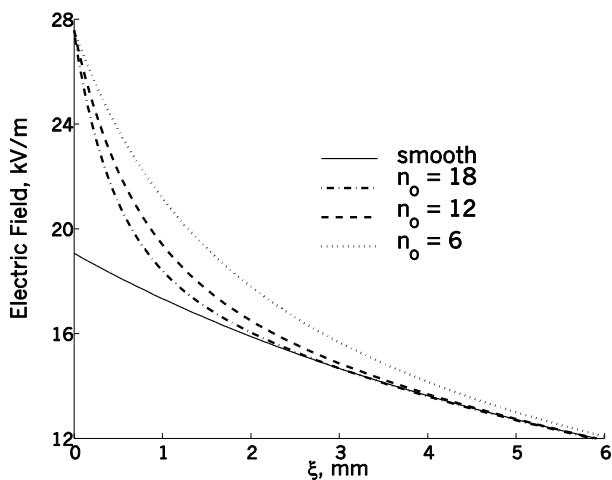

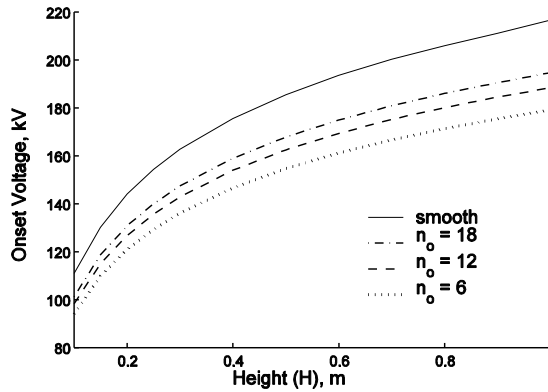Figure 7: Electric field distribution for smooth and stranded conductors, (V = 1 kV,R = 10 mm and H = 1 m).

Figure 8: Onset voltage of corona for smooth and stranded conductors
for R = 10 mm.

Figure 10 shows the increase of the calculated and measured onset voltage
values with increasing gap height H for 7- strand conductors having radii 1,
1.25 and 1.5 mm. The calculated onset voltage values agreed with those
measured experimentally within 7 %.
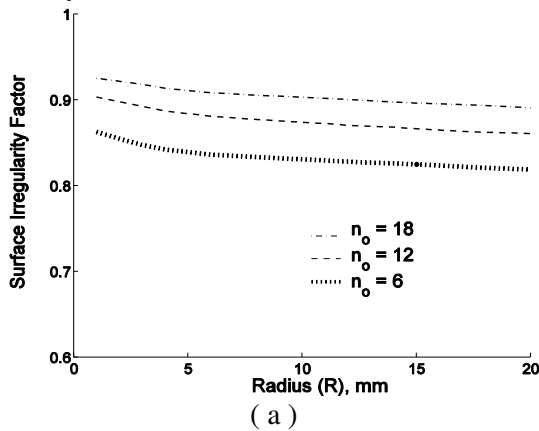
(a)
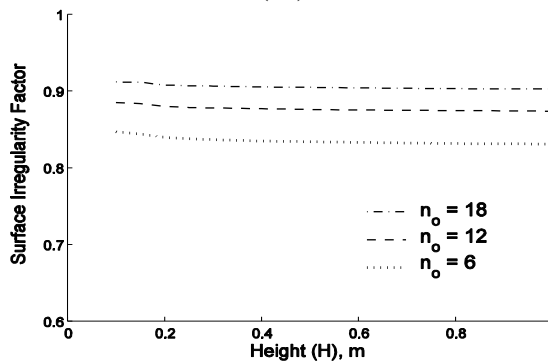
(b)

Figure 9: Predicted surface irregularity factor, m, for n_o = 6, 12 and 18;
(a) the variation of m as function of conductor radius R at gap height H = 1m.
(b) the variation of m as function of gap height H at conductor radius R = 10 mm.

Also, the calculated and measured onset voltages are compared with those estimated by Peek [6] and Lowke et al [4] formulae, at the maximum value of m (= 0.82) which was assumed before by Peek [6]. As shown in figure, most of the measured values lie over the onset values calculated by Peek's and Lowke et al formulae. The calculated data seem to be in good agreement with experimental data in comparison with the data obtained from the empirical equations.

Unlike the empirical formulae, the present method has definite values of surface irregularity factor, m and onset voltage of the corona.
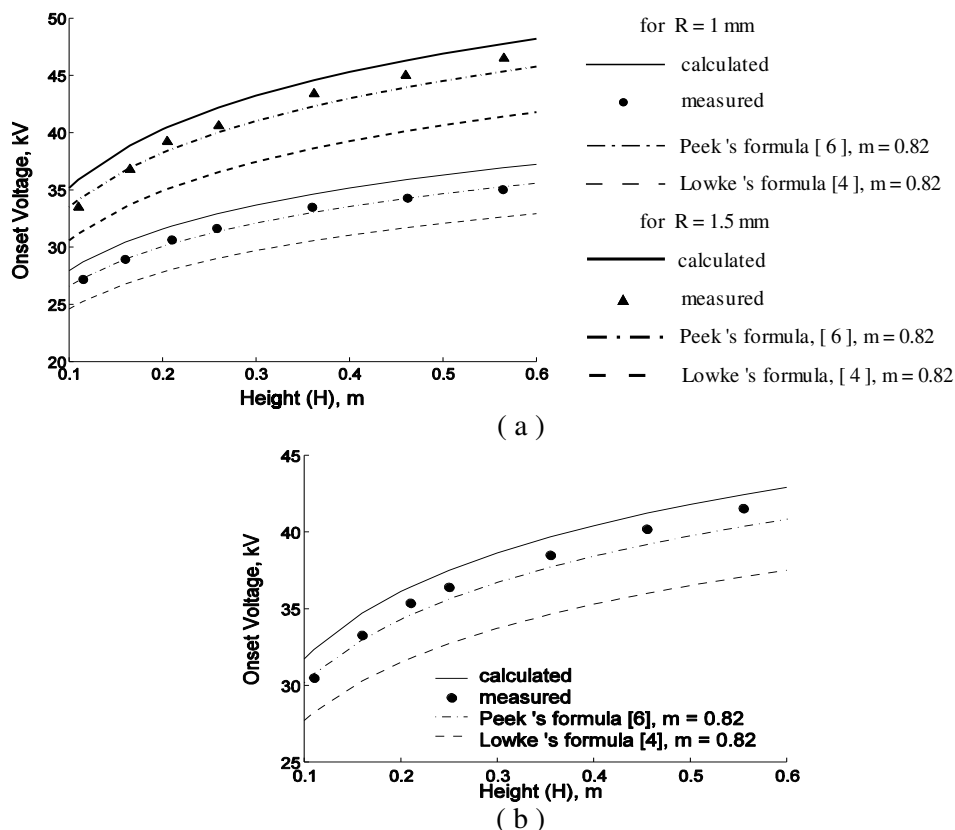

(a)

(b)

Figure 10: Measured and calculated onset voltage of corona for 7-strand
conductors having radii 1 and 1.5 mm (a) , 1.25 mm (b).

7. CONCLUSIONS

1. Electric field distribution in stranded conductors - to - plane gaps is a three-dimensional field problem. The electric field is calculated using charge simulation technique, where, the stressed conductor is simulated by a number of helical charges.

2. To achieve good accuracy, it was found that: the effective number of pitches depends on the gap height but it doesn't depend on conductor radius and type of stranding.

3. The accuracy of simulation is satisfied; the potential and the field deviation angle errors don't exceed 0.07% and 3.4 degrees over the effective conductor surface, respectively.

4. The maximum values of the surface electric field for stranded conductors divided by the maximum value of a smooth round conductor having the same radius are nearly independent of strands number n_o in the outer layer and equal approximately 1.4. This value agrees well with the values reported in the literature.

5. The larger value of n_o, the smaller the region over which the electric field deviates from that of a smooth conductor in the vicinity of conductor. Therefore, the onset voltage value increases and approaches that of a smooth round conductor as n_o increases.

6. The calculated onset voltage values agreed with those measured experimentally within 7 %.

REFERENCES

1. K. Yamazaki, and R. G. Olsen, " Application of a corona onset criterion to calculation of corona onset voltage of stranded conductors ", IEEE Transactions on Dielectrics and Electrical Insulation, Vol. 11, No. 4, pp. 674-680, August 2004.

2. S. K. Nayak and M. J. Thomas, " An integro-differential equation technique for the computation of radiated EMI due to corona on HV power transmission lines ", IEEE Transactions on Power Delivery, Vol.20, No. 1, January 2005.

3. J. Arrillaga,"*High Voltage Direct Current Transmission*", IEE Power Engineering Series, London, UK, 1998.

4. J. J. Lowke and F.D. Alessandro, "Onset corona fields and electrical breakdown criteria", Journal of Physics D: Applied Physics, Vol. 36, pp. 2673-2682, 2003.

5. M. Abdel-Salam and D. Shamloul, " Computation of ion flow fields of ac coronating wires by charge simulation techniques", IEEE Transactions on Electrical Insulation, Vol. 27, No. 2, pp. 352-361, April 1992.

6. F.W. Peek, "*Dielectric Phenomena in High Voltage Engineering*", Mc-Graw-Hill, New York, 1929.

7. J.B. Whitehead, "The electric strength of air, II ", AIEE Trans., Vol. 28, Pt. III, pp.1857-1887, 1911.

8. M. Vygodsky, "*Mathematical Handbook-Higher Mathematics*", Mir Publishers, Moscow, 1971.

9. EL-Sewedy Industries, "Egytech Cables", Cairo, Egypt, 2006.

10. D.Utmischi, "Charge substitution method for three-dimensional high voltage fields", Third International Symposium on High Voltage Engineering, Milan, August 28-31, 1979

11. Mohamed Badawi Sayed Ahmed, "Onset voltage of negative corona on stranded conductors", M. Sc. Thesis, Faculty of Engineering, Banha University, 2007.

12. M. M. El-Bahy and M. A. Abou El-Ata "Onset voltage of negative corona on dielectric-coated electrodes", Journal of Physics D: Applied Physics Vol. 38, No. 18, September 2005.

13. M. Abdel-Salam, H. Anis, A. El-Morshedy, and R. Radwan, "*High Voltage Engineering-Theory and Practice*", 2nd edition, New York: Dekker, pp.149-184, 2000.

14. M. Abdel-Salam and Dennis Wiitanen, "Calculation of corona onset voltage for duct-type precipitators" , IEEE Trans. on Industry Applications, Vol. 29, No. 2, pp. 274-280, March/April 1993.

15. M. Abdel-Salam, A. Turky and A. Hashem, "The onset voltage of coronas on bare and coated conductors", Journal of Physics D: Applied Physics Vol.31, 2550-2556, 1998.

16. N. H. Malik, " A review of the charge simulation method and its applications", IEEE Transactions on Electrical Insulation, Vol. 24, No.1, pp. 3-14, February, 1989.

17. K.S. Lyer and K.P.P. Pillai, "Analysis of irregularity factor of stranded conductor", Proc. IEE, Vol. 115, pp. 364-367, 1968.

18. G. E. Adams, "Voltage gradients on high voltage transmission lines", AIEE Transactions, Vol. 74, Pt. III, pp. 5-11, 1955.

جهد بدء التفريغ الهالى السالب على الموصلات المجدولة

فى هذا البحث تم حساب المجال الكهربى بالقرب من الموصلات المجدولة باستخدام طريقة تمثيل الشحنات حيث تم تمثيل الموصل بشحنات لولبية وضعت داخل طبقته الخارجية ، وقسم الموصل إلى عدد لانهائى من الأجزاء المتماثلة وفى كل جزء تدور الطبقة الخارجية دورة كاملة حول الموصل وفيه تقسم الشحنة اللولبية إلى شحنات خطية وبذلك يكون حساب المجال الكهربى فى الأبعاد الثلاثة ، وكانت نتيجة تمثيل الشحنات دقيقة لدرجة أن نسبة الخطأ فى حساب الجهد وزاوية إنحراف المجال على سطح الموصل لم يتعدى % 0.07 ، 3.4 درجه على التتابع وذلك للموصلات 37 ,19 ,7 المجدولة

ذات الأقطار العملية ووجد أن حساب المجال على سطح هذه الموصلات تقريبا متساوى ولا يعتمد على عدد الأسلاك فى الموصل المجدول (يساوي تقريبا 1.4 من قيمة المجال على سطح الموصل المستدير الأملس بنفس نصف القطر) بينما يختلف المجال الكهربى لهذه الموصلات بالقرب من سطح الموصل فكلما كثر عدد أسلاك الطبقة الخارجية كلما إنخفض المجال بالقرب من سطح هذه الموصلات واقترب من قيمةالمجال علي سطح الموصل الأملس المستدير ، وتم حساب جهد بدء التفريغ الهالى السالب والذى يصاحبه إستمرارية نمو الإنهمار الإلكترونى بجوار سطح الموصل ، وتم قياس حهد البدء عن طريق ظهور أول نبضة على كاشف الذبذبات، وقد أتفقت النتائج المعملية مع الحسابات النظرية بنسبة خطأ لم تتعدى 7% .